

Momentum density and Fermi surface of $\text{Nd}_{2-x}\text{Ce}_x\text{CuO}_{4-\delta}$

A. Shukla

Département de Physique de la Matière Condensée, Université de Genève, 24 quai Ernest Ansermet, CH-1211 Genève 4, Switzerland

B. Barbiellini

Laboratory of Physics, Helsinki University of Technology, SF-02150 Espoo, Finland

L. Hoffmann and A. A. Manuel

Département de Physique de la Matière Condensée, Université de Genève, 24 quai Ernest Ansermet CH-1211 Genève 4, Switzerland

W. Sadowski

Department of Physics and Mathematics, Technical University of Gdansk, ul. Majakowskiego 11/12, PL-80-952 Gdansk, Poland

E. Walker and M. Peter

Département de Physique de la Matière Condensée, Université de Genève, 24 quai Ernest Ansermet, CH-1211 Genève 4, Switzerland

(Received 12 October 1995)

High-temperature positron two-dimensional angular correlation of annihilation radiation (2D-ACAR) measurements have recently been successfully applied to map parts of the Fermi surface of $\text{YBa}_2\text{Cu}_3\text{O}_{7-\delta}$. Using the same principle, we have been able to observe with a bulk sensitive method, the Fermi surface of $\text{Nd}_{2-x}\text{Ce}_x\text{CuO}_{4-\delta}$. Although positron trapping by defects and correlation effects are strong, positron 2D-ACAR measurements provide a signal from the Fermi surface which agrees with band-structure calculations, confirming earlier surface sensitive photoemission experiments.

$\text{Nd}_{2-x}\text{Ce}_x\text{CuO}_{4-\delta}$ (NCCO) with an optimal superconducting transition temperature T_c of 25 K at a Ce concentration of $x \approx 0.15$ is a particularly interesting member of the high- T_c superconductor family. The unit cell contains a single Cu-O plane perpendicular to the c -axis with Nd atoms directly above and below the Cu atom. One characteristic of NCCO is that it is the only electron-doped high- T_c superconductor, with Ce^{4+} ions substituting Nd^{3+} ions. The calculated band structure of NCCO (Ref. 1) leads to a single free-electron-like band crossing the Fermi energy E_F and producing a simple, highly two-dimensional Fermi surface (FS). According to Massidda *et al.*¹ the density of states at E_F is smaller than in other high- T_c superconductors and this might mean that the Fermi edge will be weaker in this material. In the experimental search for the FS of high- T_c superconductors, NCCO has also been investigated and a major breakthrough was the identification of its FS simultaneously by two groups^{2,3} using angle-resolved photoemission spectroscopy (ARPES). They came to the conclusion that the observed FS is in close agreement with the calculations.¹

Positron two-dimensional angular correlation of annihilation radiation (2D-ACAR) has been used to study the electronic structure and Fermiology of high- T_c superconductors.⁴ These efforts have been hampered by sample quality and weak signals but have nevertheless led to important results, notably the identification of the FS due to the copper-oxygen "chain" structure in $\text{YBa}_2\text{Cu}_3\text{O}_{7-\delta}$.⁵ However, in most high- T_c superconductors the highly anisotropic structure leads to an inherent limitation for 2D-ACAR because positrons, repulsed by atomic cores, sample interstitial space preferentially. In $\text{YBa}_2\text{Cu}_3\text{O}_{7-\delta}$, for example, the positron density distribution is concentrated in the layer containing

the chains and the FS signal due to the copper-oxygen planes cannot be observed by 2D-ACAR. Since high- T_c superconductivity is thought to originate in the planes any information from this region is valuable. Calculations⁶ have shown that in NCCO positrons are more homogeneously distributed and in principle the FS signal should be observed by 2D-ACAR. An earlier measurement performed at a temperature $T=10$ K,⁶ however, failed to observe any such signal. Meanwhile, we have conducted an in-depth study of the mechanisms of positron trapping in $\text{Y}_{1-x}\text{Pr}_x\text{Ba}_2\text{Cu}_3\text{O}_{7-\delta}$ using positron lifetime spectroscopy^{7,8} and concluded that 2D-ACAR measurements performed at $T=400$ K should not contain contributions from trapped positrons in this material. Spectra measured in such conditions fulfilled this expectation and revealed an additional chain-related FS.⁹ With this in mind we undertook to measure the 2D-ACAR spectrum of NCCO at $T=400$ K. In this paper, we present these high-temperature measurements and also calculations of the electron-positron momentum density. We discuss the comparison between experiment and theory, showing that despite some positron trapping by defects we observe the Fermi surface and find its topology in good agreement with band-structure calculations.

Our calculations are based on the linear muffin-tin orbital (LMTO) method which includes electron-positron correlation within the generalized gradient approximation (GGA). Owing to the strong electron-positron correlation, the electron density at the site of the positron is enhanced by a factor $\gamma(r)$. The positron annihilation rate λ , which is the inverse of the positron lifetime τ , is calculated from the overlap of the positron and the electron densities according to

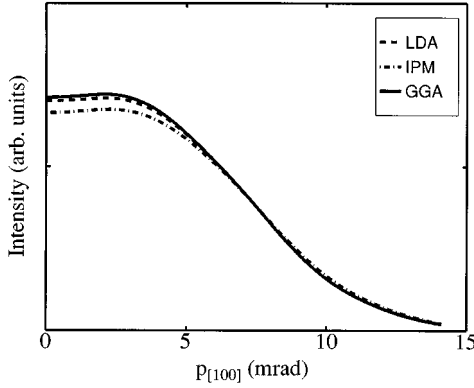


FIG. 1. Sections through the center of theoretical 2D-ACAR spectra from NCCO convoluted with the experimental resolution function. Inclusion of positron-electron correlation induces an enhancement and leads to more peaked 2D-ACAR curves. However, both GGA and LDA are quite alike.

$$\lambda = \pi r_e^2 c \int n_+(r)n_-(r)\gamma(r)d^3r, \quad (1)$$

where r_e is the classical electron radius and c is the speed of light. In the local density approximation (LDA),¹⁰ $\gamma(r)$ is treated as a function of the electron density $n(r)$. However, the LDA based on the Arponen and Pajanne uniform electron gas calculations¹¹ overestimates $\gamma(r)$ thus underestimating positron lifetimes, especially when localized electrons are involved. This problem can be cured by the GGA for electron-positron correlation.¹² In the GGA, $\gamma(r)$ depends also on the density gradient $\nabla n(r)$, reducing the value of $\gamma(r)$.

The electron-positron momentum density $\rho^{2\gamma}$ is calculated from

$$\rho^{2\gamma}(\mathbf{p}) = \sum_{n,\mathbf{k}}^{\text{occ}} \left| \int e^{-i\mathbf{p}\cdot\mathbf{r}} \psi_{n\mathbf{k}}(\mathbf{r}) \psi_+(\mathbf{r}) \sqrt{\gamma(\mathbf{r})} d\mathbf{r} \right|^2, \quad (2)$$

where $\psi_{n\mathbf{k}}$ and ψ_+ are the (occupied) electron and positron wave functions and where n and \mathbf{k} label the band and \mathbf{k} -point, respectively. To correct the overlapping spheres of the LMTO method, we have used the method described by Singh and Jarlborg.¹³ The agreement with the corresponding full-potential linear augmented-plane-wave results is very good.⁶

The effect of γ is to enhance the annihilation in the interstitial space (where the electron density is smaller) and the gradient correction increases this trend. Therefore, the GGA yields more localized annihilation in the momentum space. This trend is shown in Fig. 1 where a line through the once-integrated $\rho^{2\gamma}(\mathbf{p})$ is presented. It is in better agreement with the experiment. Since our momentum density calculations are only valid for positrons in delocalized states, deviations from the experiment might also be due to annihilations of positrons localized in defects. It is therefore important to consider these trapping effects in details.

The measurement of the positron lifetime is a valuable test for the presence of positron traps. In NCCO, Howell *et al.*¹⁴ measured a lifetime of about 200 ps without temperature dependence. Blandin *et al.*⁶ reported a similar value in

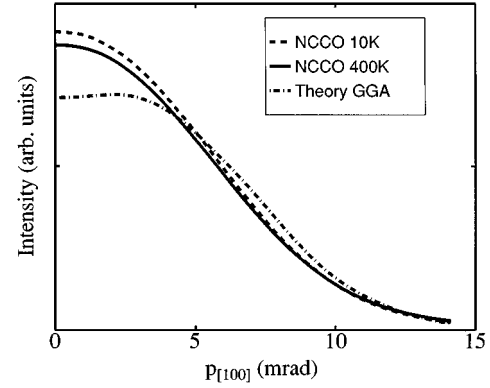


FIG. 2. Sections through the center of 2D-ACAR distribution from NCCO normalized to the same volume. The difference between the measurements at 10 and 400 K is attributed to shallow traps whereas comparison with theory may be aggravated by trapping in deep metallic traps.

the 100–300 K range and did not see any difference between insulating and superconducting compounds. Sundar *et al.*¹⁵ report values between 205 and 230 ps, depending on the concentration of oxygen. These experimental values have to be compared with lifetimes of 112 ps (LDA) and 148 ps (GGA) calculated by LMTO. The larger experimental lifetimes suggest that positrons are trapped by defects in the samples. As the complexity of self-consistent calculations increases when vacancies are introduced in the system, we have used the non-self-consistent scheme of free-atom superposition¹⁰ to calculate lifetimes both in the perfect lattice and in defects. In this scheme, the NCCO bulk lifetime is 131 ps in the LDA and 165 ps in the GGA and for the ideal Cu, Nd, O1, and O2 vacancies, one obtains, respectively, lifetimes of 172, 199, 134, and 137 ps in the LDA and 220, 268, 170 and 172 ps in the GGA.¹⁶ Our measured lifetime (204–207 ps) (Ref. 6) is similar to the one calculated for copper vacancies in the GGA. This suggests the presence of this defect in the real samples. However, the lifetime spectrum could also contain contributions from positrons annihilating in oxygen vacancies, as it is not possible to resolve experimentally two lifetimes which differ by 20–30 ps. Moreover, the binding at the oxygen vacancies is very weak¹⁶ and, therefore the positron trapping at the oxygen vacancies is a good explanation of the temperature dependence observed in the ACAR spectra.

The 2D-ACAR distribution is the once-integrated electron-positron momentum density $\rho^{2\gamma}$ given in Eq. (2). The measurements were performed with the c axis aligned to the direction of projection. The experimental setup has been described earlier.¹⁷ We have used a $\text{Nd}_{2-x}\text{Ce}_x\text{CuO}_{4-\delta}$ single crystal grown by a flux technique.¹⁸ The crystal of roughly $3 \times 3 \text{ mm}^2$, had a $T_c = 17 \text{ K}$ and $\Delta T_c = 2 \text{ K}$. The Ce concentration can be estimated to be $0.13 \leq x \leq 0.16$ and is very critical to form the superconducting phase. We had previously measured the 2D-ACAR spectrum from NCCO (Ref. 6) at 10 K with a statistics of 1.1×10^8 counts. This measurement will be referred to as NCCO 10 K. Since NCCO 10 K had not revealed any FS we decided to measure at $T = 400 \text{ K}$ in the hope of detraping positrons that might be trapped in any shallow traps. This measurement will be referred to as

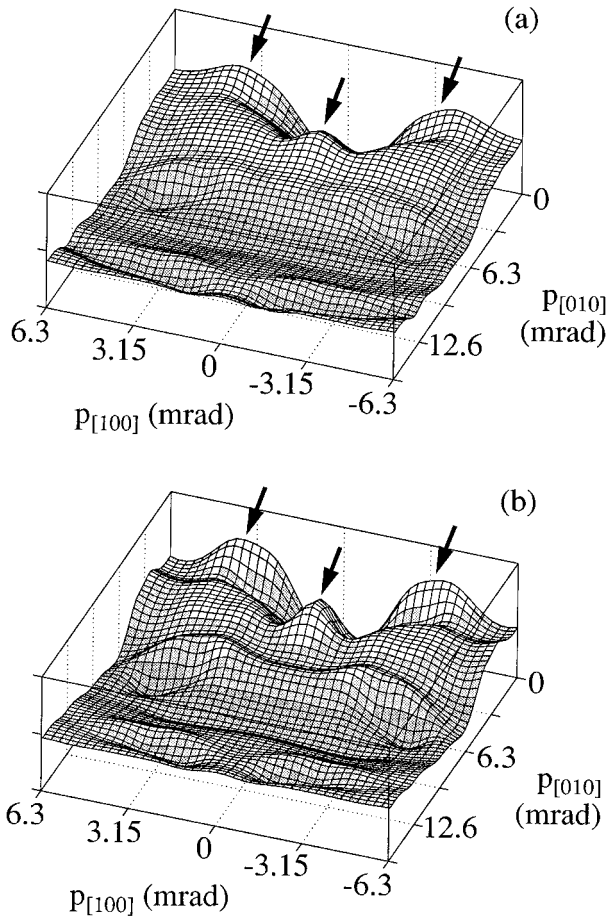


FIG. 3. Bandpass filtered 2D-ACAR of NCCO calculated from LMTO within the independent particle model (a), and by including electron-positron correlation within GGA (b). The arrows points to the main structures relating to the Fermi surface.

NCCO 400 K. The statistics is 5.7×10^8 counts. In Fig. 2 one observes the difference, attributed to shallow positron trapping, between NCCO 10 K and NCCO 400 K. However, the theoretical curve is much broader indicating that the major trapping sites for positrons in NCCO are probably deep traps.

Though we have not measured the lifetime at 400 K, we can compare the value for the S factor at 10 K and 400 K. We define a slice 1.95 mrad wide and stretching 13.1 mrad on either side of the maximum of the 2D-ACAR spectrum along the $p_{[100]}$ or $p_{[010]}$ directions. The S factor is the ratio of the counts contained in a central core (of total length 7.35 mrad) of this slice to the total counts in the slice. Trapped positron sample preferentially delocalized electrons and, in momentum space, this results in a narrowing of the 2D-ACAR distribution and a larger S parameter. For NCCO we find $S=0.5159$ and 0.5094 at 10 and 400 K, respectively. Because error on these values is less than 5×10^{-4} it is clear that the positron is more delocalized in the high-temperature measurement. The amount of anisotropy in 2D-ACAR spectra is an indication of the contribution from valence electrons to the total annihilation. The anisotropic part of the 2D-ACAR spectrum is extracted by subtracting a cylindrical average from the data and the ratio of the maximum amplitude

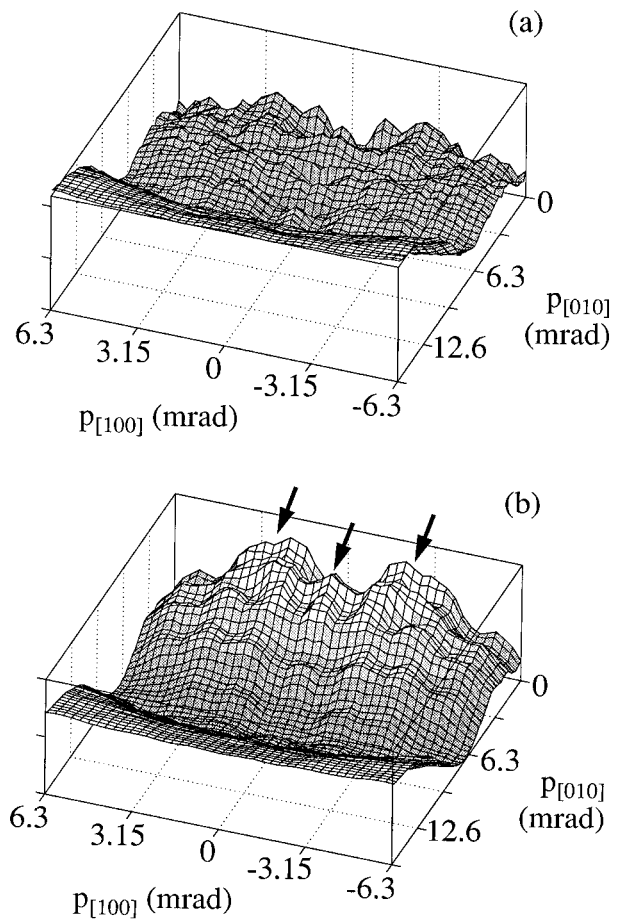


FIG. 4. Bandpass filtered 2D-ACAR measured from NCCO at 10 K (a) and 400 K (b). Structure appears in the high-temperature measurement and compares well with theoretical results shown in Fig. 3.

of this part to the maximum of the 2D-ACAR spectrum is then a measure of anisotropy. We find a value of 2.7% for NCCO 400 K and 3.1% for the theoretical spectrum. This indicates that the proportion of valence to core annihilations in the experiment is similar to that assumed in theory. However, one must keep in mind that the theoretical and experimental spectra do not yet agree very well and that in high- T_c superconductors the anisotropy in 2D-ACAR spectra is often dominated by wave-function effects.

To analyze the 2D-ACAR, which are very isotropic in nature, we use bandpass filtering.¹⁹ We wish to extract small signals superposed on a large bell-shaped background originating from annihilations with electron states in filled bands and from positrons trapped in defects. The filtering operation consists of two parts: a heavily smoothed 2D-ACAR spectrum is subtracted from the original spectrum. The residual difference is then weakly smoothed to remove statistical noise. Filtered 2D-ACAR spectra for theory and experiment are shown in Figs. 3 and 4. The theoretical spectra show features which are associated with the FS, notably those marked with the arrows. These signals are generated by the single band crossing the FS and reflect the Fermi breaks in the electron momentum distribution. In the GGA model [Fig. 3(b)], although there are modulations produced by the corre-

lation factor γ , the FS breaks are still clear, allowing their experimental detection. In NCCO 10 K [Fig. 4(a)] there is no distinguishable feature in the filtered spectrum. In NCCO 400 K [Fig. 4(b)], the filtered spectrum shows stronger resemblance with theory. The partial delocalization of the positrons at high temperature has improved the comparison significantly. In particular, features corresponding to the FS appear. Though it is weak, the signal is seen over a region of about 2 mrad (1 mrad = 0.137 a.u. of momentum), which is more than twice the distance over which data are correlated by the filtering procedure. The result obtained through bandpass filtering has been confirmed using the Lock-Crisp-West (LCW) (Ref. 20) folding procedure, which consists in reducing the 2D-ACAR within the first Brillouin zone. The result can be related to the electron occupation number. As trapping and wave-function effects bias the reduced distribution, we have applied the LCW procedure to the anisotropic part of the 2D-ACAR. To enhance the contrast, the LCW data were smoothed and subtracted from its isotropic background. The same procedure was applied to the theory. The results agree reasonably well and confirm the finding from bandpass filtering.

As stated above, we believe that positron trapping in deep traps is present in NCCO and is the main reason for persisting differences between theory and experiment. Nevertheless, there are other possibilities. The first could be an inferior quality of our samples, for example, the presence of a substantial amount of the insulating phase. Another possibil-

ity might be related to the relatively low T_c of our sample (17 K with $\Delta T_c = 2$ K) with respect to the optimal value (25 K). Photoemission studies^{2,3} indicate that this can hinder the observation of the FS. Finally, it might also be that the absence of the one-band FS signal at low temperature, if not the consequence of shallow trapping of positrons, could be related to a change of sign of the carriers, as suggested by transport property measurements in samples having $T_c = 17$ K.²¹ In the low-temperature regime, the electronic properties of NCCO would then be governed by a two-conduction-band picture induced by the buckling of the CuO_2 planes.²¹ At present, we are not able to determine if our low-temperature data are compatible with this model.

In conclusion, 2D-ACAR is a bulk experimental technique to provide indications of a Fermi surface in the n -doped cuprate $\text{Nd}_{2-x}\text{Ce}_x\text{CuO}_{4-\delta}$. This is significant because this Fermi surface is due to the copper-oxygen planes, where superconductivity is thought to occur. The signal, however, is weaker than in the theory, mainly due to the partial trapping of positrons by defects. Our positron annihilation studies suggest that the shape of the Fermi surface of $\text{Nd}_{2-x}\text{Ce}_x\text{CuO}_{4-\delta}$ is well described by band theory, like it was for the case of the high- T_c superconductors previously studied.⁴ Our results also confirm surface-sensitive ARPES experiments.^{2,3}

We are grateful to the Swiss National Science Foundation for its financial support.

-
- ¹S. Massidda, N. Hamada, J. Yu, and A. J. Freeman, *Physica C* **157**, 571 (1989).
- ²R. O. Anderson, R. Claessen, J. W. Allen, C. G. Olson, C. Janowitz, L. Z. Liu, J.-H. Park, M. B. Maple, Y. Dalichaouch, M. C. de Andrade, R. F. Jardim, E. A. Early, S.-J. Oh, and W. P. Ellis, *Phys. Rev. Lett.* **70**, 3163 (1993).
- ³D. M. King, Z.-X. Shen, D. S. Dessau, B. O. Wells, W. E. Spicer, A. J. Arko, D. S. Marshall, J. DiCarlo, A. G. Loeser, C. H. Park, E. R. Ratner, J. L. Peng, Z. Y. Li, and R. L. Greene, *Phys. Rev. Lett.* **70**, 3159 (1993).
- ⁴A. A. Manuel, A. Shukla, L. Hoffmann, T. Jarlborg, B. Barbiellini, S. Massidda, W. Sadowski, E. Walker, A. Erb, and M. Peter, *J. Phys. Chem. Solids* (to be published).
- ⁵H. Haghghi, J. H. Kaiser, S. Rayner, R. N. West, J. Z. Liu, R. Shelton, R. H. Howell, F. Solar, P. A. Sterne, and M. J. Fluss, *J. Phys. Chem. Solids* **52**, 1535 (1991); *Phys. Rev. Lett.* **67**, 38 (1991).
- ⁶P. Blandin, S. Massidda, B. Barbiellini, T. Jarlborg, P. Lerch, A. A. Manuel, L. Hoffmann, M. Gauthier, W. Sadowski, E. Walker, M. Peter, J. Yu, and A. J. Freeman, *Phys. Rev. B* **46**, 390 (1992).
- ⁷A. Shukla, L. Hoffmann, A. A. Manuel, B. Barbiellini, M. Peter, and E. Walker, *Mater. Sci. Forum* **175-178**, 929 (1995).
- ⁸A. Shukla, Ph.D. thesis, University of Geneva, 1995.
- ⁹A. Shukla, L. Hoffmann, A. A. Manuel, E. Walker, B. Barbiellini, and M. Peter, *Phys. Rev. B* **51**, 6028 (1995).
- ¹⁰M. J. Puska and R. M. Nieminen, *Rev. Mod. Phys.* **66**, 841 (1994).
- ¹¹J. Arponen and E. Pajanne, *Ann. Phys. (N.Y.)* **121**, 343 (1979).
- ¹²B. Barbiellini, M. J. Puska, T. Torsti, and R. M. Nieminen, *Phys. Rev. B* **51**, 7341 (1995).
- ¹³A. K. Singh and T. Jarlborg, *J. Phys. F* **15**, 727 (1985).
- ¹⁴R. H. Howell, H. B. Radousky, A. L. Wachs, M. J. Fluss, P. E. A. Turchi, Y. C. Jean, C. S. Sundar, C. W. Chu, J. L. Peng, T. J. Folkerts, R. N. Shelton, and D. G. Hinks, *Physica C* **162-164**, 1377 (1989).
- ¹⁵C. S. Sundar, A. Bharathi, Y. C. Jean, P. H. Hor, R. L. Meng, Z. J. Huang, and C. W. Chu, *Phys. Rev. B* **42**, 426 (1990).
- ¹⁶B. Barbiellini, M. J. Puska, A. Harju, and R. M. Nieminen, *J. Phys. Chem. Solids* (to be published).
- ¹⁷P. E. Bisson, P. Descouts, A. Dupanloup, A. A. Manuel, E. Péréard, M. Peter, and R. Sachot, *Helv. Phys. Acta* **55**, 100 (1982).
- ¹⁸W. Sadowski, M. Affronte, M. Francois, E. Koller, and E. Walker, *J. Less Common Met.* **164 & 165**, 824 (1990).
- ¹⁹K. M. O'Brien, M. Z. Brand, S. Rayner, and R. N. West, *J. Phys. Condens. Matter* **7**, 925 (1995).
- ²⁰D. G. Lock, V. H. C. Crisp, and R. N. West, *J. Phys. F* **3**, 561 (1973).
- ²¹Wu Jiang, S. N. Mao, X. X. Xi, Xiuguang Jiang, J. L. Peng, T. Venkatesan, C. J. Lobb, and R. L. Greene, *Phys. Rev. Lett.* **73**, 1291 (1994).